ELSEVIER

Biophysical Chemistry 91 (2001) 157–166

Biophysical Chemistry

www.elsevier.com/locate/bpc

Noise enhanced hormonal signal transduction through intracellular calcium oscillations

Leonhard Läer[a], Mirko Kloppstech[a], Christof Schöfl[a], Terrence J. Sejnowski[b,c], Georg Brabant[a], Klaus Prank[a,*]

[a] *Computational Endocrinology Group, Department of Clinical Endocrinology, Medical School Hannover, D-30623 Hannover, Germany*

[b] *Computational Neurobiology Laboratory, Howard Hughes Medical Institute, Salk Institute for Biological Studies, San Diego, CA 92186-5800, USA*

[c] *Department of Biology University of California, San Diego, La Jolla, CA 92093, USA*

Received 2 January 2001; received in revised form 9 April 2001; accepted 11 April 2001

Abstract

In a wide range of non-linear dynamical systems, noise may enhance the detection of weak deterministic input signals. Here, we demonstrate this phenomenon for transmembrane signaling in a hormonal model system of intracellular Ca^{2+} oscillations. Adding Gaussian noise to a subthreshold extracellular pulsatile stimulus increased the sensitivity in the dose–response relation of the Ca^{2+} oscillations compared to the same noise signal added as a constant mean level. These findings may have important physiological consequences for the operation of hormonal and other physiological signal transduction systems close to the threshold level.

Keywords: Stochastic resonance; Non-linear dynamical systems; Pulsatile hormone secretion; Calcium oscillations; Calcium signaling

1. Introduction

The exchange of biological information between distant cells or organs is achieved by two major systems: the nervous and the endocrine system. In the nervous system information is encoded in the temporal pattern of neuronal spike trains [1]. The specificity of information transfer arises from the architecture of the neuronal network. On the other hand, in the endocrine system, information is unspecifically transmitted via the blood stream. The specificity of signaling arises from the biochemical structure of the hormones and their respective receptors [2]. Most hormones are not

* Corresponding author. BIOBASE Biological Databases/Biologische Datenbanken GmbH, Mascheroder Weg 1b, D-38124 Braunschweig, Germany. Tel.: +49-531-260-3624; fax: +49-531-260-3670.

E-mail address: klaus.prank@biobase.de (K. Prank).

0301-4622/01/$ - see front matter
PII: S0301-4622(01)00167-3

constantly released into the blood stream but in a burst-like, pulsatile manner [3,4]. This temporal pattern of hormone secretion has been shown to specifically regulate many distinct cellular functions [5–7].

The Ca^{2+}-phosphatidylinositol (PI) signaling pathway plays a major role in transmembrane signaling in a large number of different cell types [8]. In this pathway, hormonal stimuli lead to the activation of G-proteins as an effector system

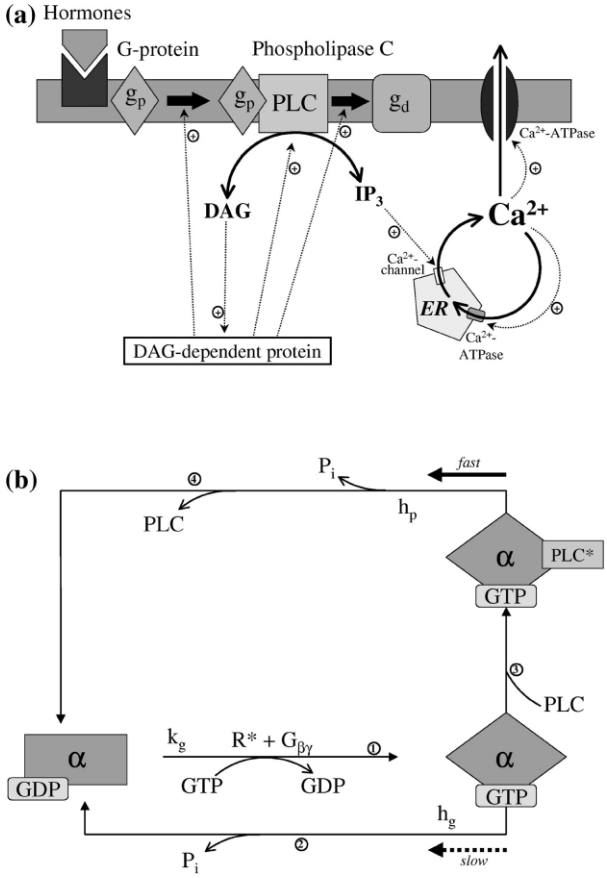

Fig. 1. (a) Generation of intracellular Ca^{2+}-oscillations in electrically non-excitable cells. Here, g_p stands for the G_α-GTP, g_d for G_α-GDP, PLC for phospholipase C, IP_3 for inositol(1,4,5)-trisphosphate, DAG for diacylglycerol, and ER for the endoplasmic reticulum. The dotted lines mark feedback. (b): In the modified Bourne–Stryer mechanism, phospholipase C acts as a protein activating G_α-GTP. The square is an inactive form and the diamond is an active form of G-protein α-subunit bound to GDP and GTP, respectively. GDP stands for guanosine-5′-diphosphate, and GTP stands for guanosine-5′-triphosphate. PLC is an effector which becomes active (PLC*) when it is bound to G_α-GTP. The exchange of GTP for bound GDP is catalyzed by the hormone–receptor complex, R*, with the help of the βγ-subunit of G-protein (step 1). Hydrolysis of the bound GTP brings the G-protein back to the inactive state (step 2). This hydrolysis step is a very slow step. On the other hand, G_α-GTP activates the effector protein, PLC (step 3). GTP hydrolysis by G_α-GTP complexed with PLC is much faster than that of G_α-GTP alone, i.e. step 4 is faster than step 2. (Fig. 1 is a modification of an already published illustration in Chay et al. [16]). The model we use is based on these four steps and is summarized as follows (see Section 2): PLC* is the GTP-ase activating protein; PLC* is formed when 4 mol of G_α-GTP is combined with PLC; PLC* is an effector which can produce IP_3 and diacylglycerol (DAG) from phophatidylinositol(4,5)-biphosphate (PIP_2); Steps 3 and 4 are enhanced by a DAG-dependent protein. The production of DAG and IP_3 by PLC* is also enhanced by the same protein. The enhancement of these steps by a DAG-dependent protein is necessary to generate the oscillation. However, to generate the oscillation, the DAG-dependent protein can be replaced by a Ca^{2+}-dependent protein or by a protein which is activated by both $[Ca^{2+}]_i$ and [DAG].

which subsequently activates the enzyme phospholipase C (PLC). The activated enzyme PLC then results in the formation of the second messenger substances inositol 1,4,5-trisphosphate (IP_3) and 1,2-diacylglycerol (DAG) from phophatidylinositol 4,5-bisphosphate (PIP_2). IP_3 triggers the release of Ca^{2+} from internal stores, such as the endoplasmic reticulum (ER). Succeeding feedback mechanisms lead to a fall of the intracellular calcium concentration ($[Ca^{2+}]_i$) back to resting levels. This is achieved through the enhancement of active transport mechanisms via Ca^{2+}-ATPases like pumping Ca_i^{2+} back into the internal stores and out of the cell and by temporary binding of Ca_i^{2+} through proteins (Fig. 1). The result are repetitive $[Ca^{2+}]_i$-spikes varying in frequency and amplitude depending on the strength and type of the hormonal stimulus. $[Ca^{2+}]_i$-spike trains allow for the differential regulation of distinct cellular responses [9], such as the activation of protein kinases [10] as well as the activation of genes [11], differentiation [12,13], motility, and morphology [14].

To date, the generation of $[Ca^{2+}]_i$-spikes has been studied experimentally and numerically under constant hormonal stimulation. Based on the fact that hormones are secreted in a burst-like or pulsatile manner, experiments have been performed in single hepatocytes which demonstrated the mapping of periodic pulsatile hormonal stimuli with the α_1-adrenoreceptor agonist phenylephrine into distinct temporal patterns of $[Ca^{2+}]_i$-spike trains [15]. In these experiments 1:1, 2:1 and 5:4 locking rhythms were found between the extracellular hormonal stimulus and the intracellular $[Ca^{2+}]_i$-response. Furthermore, a modulation of the $[Ca^{2+}]_i$-spike amplitude by the frequency of the periodic hormonal stimulus could be observed. Motivated by this study, a mathematical model for receptor-controlled $[Ca^{2+}]_i$-spikes was adapted [16], which had been numerically studied only under constant agonist stimulation [17]. This new model accounts for most of the dynamical features observed experimentally, such as blocked and delayed $[Ca^{2+}]_i$-responses to the extracellular stimulus [15]. Extensive simulations of this model have been performed using a large variety of different pulsatile stimuli with different interpulse intervals, pulse durations and amplitudes to explore the mapping of the dynamic stimulus pattern to the $[Ca^{2+}]_i$-spike train [16].

Numerical simulations of this model performed so far have either used constant stimuli or periodically delivered square pulses without assuming any noise in the stimulatory profile. In biological systems, the impact of noise on the enhancement of signal transduction of weak subthreshold stimuli, called stochastic resonance (SR), has been extensively studied experimentally and numerically for sensory neurons on the cellular and systems level [18–25], and on the subcellular level for an ion channel [26] and receptor cell syncytium structure [27]. This mechanism has been explained by a non-linear cooperative effect arising from the coupling between deterministic and random signals in a wide range of physical systems [21,28–34].

In biochemical systems, the effect of noise on the transduction of subthreshold stimuli has not been studied yet. In contrast to the transmission of information in the nervous system by repetitive spikes of the electrical activity of neurons, the information transfer in the hormonal system is based on the specific biochemical structure of the signaling molecules and the temporal profile of their release. Here, we use the mathematical model described above to simulate transmembrane signal transduction from extracellular fluctuating hormonal stimuli to repetitive spikes of $[Ca^{2+}]_i$ and investigate the effect of noise on the transduction of subthreshold stimuli. This non-excitable cell model is still the only one exhaustively examined driven by dynamical stimuli and found to correspond with in vitro experiments, although it would have to be modified to reflect the most recent findings.

2. Model

2.1. Mathematical model for receptor-controlled $[Ca^{2+}]_i$-oscillations

The model [16], used in this study is summarized by the following equations:

$$\frac{d[G_\alpha - GTP]}{dt} = k_g[G_\alpha - GDP] - 4k_p[G_\alpha - GTP]^4[PLC] - h_g[G_\alpha - GTP] \quad (1)$$

$$\frac{d[DAG]}{dt} = k_d[PLC^*] - h_d[DAG] + l_d \quad (2)$$

$$\frac{d[Ca^{2+}]_i}{dt} = \rho\left\{k_c\frac{[IP_3]^3}{K_S^3 + [IP_3]^3} - h_c[Ca^{2+}]_i + l_c\right\} \quad (3)$$

$$\frac{d[PLC^*]}{dt} = k_p[G_\alpha - GTP]^4[PLC] - h_p[PLC^*] \quad (4)$$

Eq. (1) describes the change of [G_α-GTP] due to the conversion of G_α-GDP to G_α-GTP (Fig. 1b). The second term describes the loss of [G_α-GTP] to build up the activated enzyme PLC (PLC*). In Eq. (1), k_g is assumed to be 'proportional' to the time-varying agonist concentration (in units of s^{-1}; see Chay et al. [16]), i.e. the concentration of the extracellular hormone. Therefore, the value of k_g could not become negative for physiological reasons.

The three kinetic parameters k_p, h_p, k_d are assumed to take the following forms:

$$k_n = k'_n\frac{[DAG]^2}{K_D^2 + [DAG]^2} \quad (5)$$

where $k_n = k_p$, h_p or k_d and $k'_p = 2 \times 10^{-7}$ nM^{-4} s^{-1}, $h'_p = 0.5$ s^{-1}, $k'_d = 700$ s^{-1}. The remaining kinetic constants are $K_D = 25$ nM and h_g which is set to 0.0 s^{-1} in a first approximation. Eq. (2) models the change of DAG and IP_3 ($h_d = 100$ s^{-1}, $l_d = 250$ nM s^{-1}) (Fig. 1a). For simplicity, it is assumed that [DAG] and [IP_3] increase with the same rate. Eq. (3) describes the change of the intracellular calcium concentration $[Ca^{2+}]_i$ ($\rho k_c = 9.0 \times 10^4$ nM s^{-1}, $K_s = 300$ nM, $\rho h_c = 1.0$ s^{-1}, $\rho l_c = 200$ nM s^{-1}). The first term in the curly brackets is a Hill function which models co-operativity for binding of IP_3 to the tetrameric receptor on the ER (endoplasmic reticulum), resulting in the release of Ca^{2+}. Since 3 M of IP_3 are required to release Ca^{2+} from the ER, the exponent 3 occurs in this equation. The second term describes a loss of $[Ca^{2+}]_i$ due to Ca^{2+}-ATPase-pumps. The third term expresses the pouring in of Ca^{2+}-ions to the cell to keep it at its basal $[Ca^{2+}]_i$-level in the absence of external stimuli. The ρ value is related to $[Ca^{2+}]_{ER}$. Eq. (4) models the formation of PLC from PLC through the action of G_α-GTP. The second term describes the loss of PLC by the hydrolysis of the complex to G_α-GDP. The exponent 4 occurs again in the first term of this equation since 4 M of G_α-GTP are required to form PLC. For a detailed explanation of all the parameters, see Chay et al. [16].

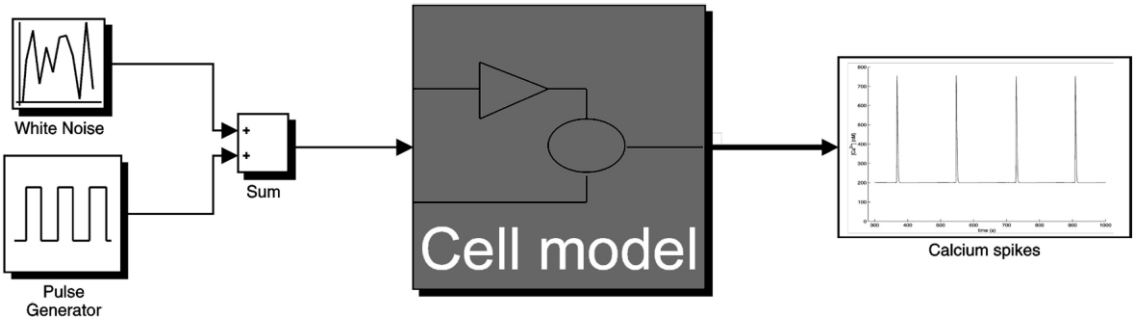

Fig. 2. Each $[Ca^{2+}]_i$-spike train, $x(t)$, was simulated for 18.000 s on a Sun SPARCstation 20 using source code written in MATLAB (MathWorks Inc., Natick, MA). The system of differential equations was integrated using a modified Rosenbrock formula stiff solver (variable integration time step).

A qualitative explanation for the generation of $[Ca^{2+}]_i$-spike trains in this model is as follows: Ca^{2+} is released from intracellular Ca^{2+}-stores (such as the ER) when $[G_\alpha\text{-GTP}]$ and thus $[IP_3]$ reach a critical threshold level. The Ca^{2+}-response is blocked when $[G_\alpha\text{-GTP}]$ is too low and the agonist stimulus is delivered prematurely. Details of the numerical simulation of this model are given in the legend of Fig. 2. To analyze the dynamic behavior of this model, we constructed a bifurcation diagram as a function of the stimulus amplitude k_g using the AUTO program (Fig. 6, [35]).

2.2. Effect of additive Gaussian noise on transmembrane signal transduction

The effect of different intensities of additive bandlimited Gaussian distributed white noise (GN) on the generation of repetitive $[Ca^{2+}]_i$-transients by periodically applied extracellular stimuli was investigated using the model described above (Fig. 3). We added the constant mean level ($\overline{GN}$) of the respective noise signal to the extracellular subthreshold stimulus as a control (Fig. 3c). The interpulse intervals used in this numerical study ranging from 30 to 180 s were chosen according to the experimental data on Ca^{2+}-signalling in hepatocytes [15]. The pulse duration was 5 s. The maximum noise amplitude was varied from 0.0 to 3.0×10^{-2} s^{-1}, corresponding to a noise variance between 0.0 and 1.5×10^{-5} s^{-2} (r.m.s.) and a corresponding mean level between 0.0 and 1.5×10^{-2} s^{-1}, which increased with the variance. In contrast to studies on stochastic resonance in sensory neurons where zero-mean noise has been added, this is not possible in our study. To add zero-mean noise would require negative values

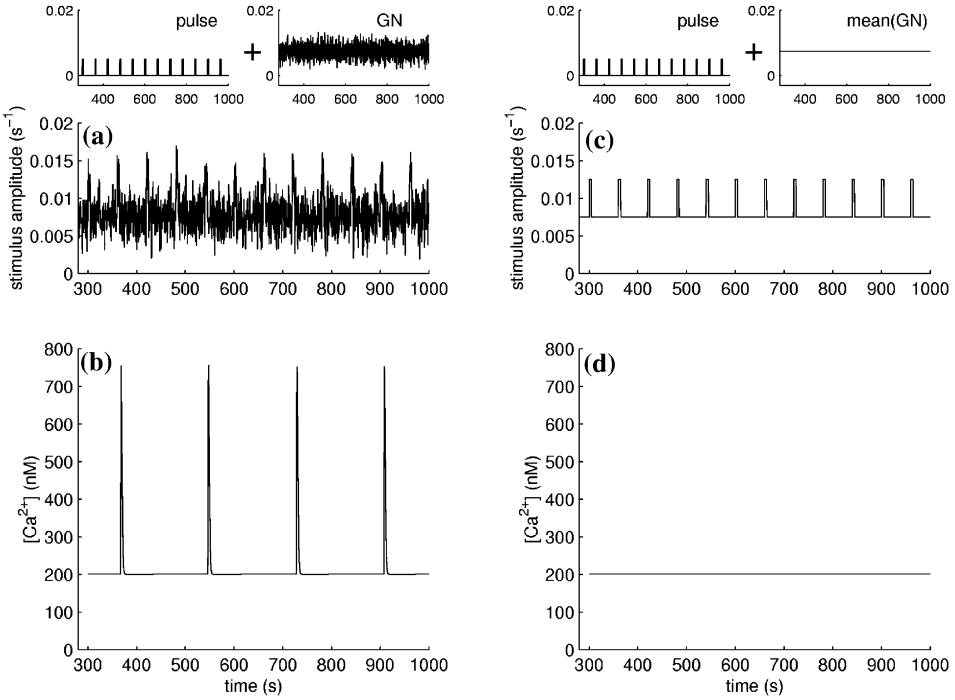

Fig. 3. Generation of pulsatile stimuli with and without Gaussian distributed noise (GN) and intracellular Ca^{2+}-responses based on Eqs. (1)–(4). The interpulse interval of the stimulus was 60 s and the pulse duration was 5 s. (a) Stimulus composed of a noiseless subthreshold pulsatile signal and input GN; (b) corresponding $[Ca^{2+}]_i$-response to the stimulus in (a); (c) stimulus composed of a noiseless subthreshold pulsatile signal with the mean level of the GN in (a) added to ($\overline{GN}$); and (d) corresponding $[Ca^{2+}]_i$-spike train to the stimulus in (c).

for the noise. Since we assume that the pulsatile stimulus plus the noise is proportional to the concentration of the agonist (rate k_g in Eq. (1)) we are restricted to values larger than or equal to zero. Before GN was added to the stimulus signal, it was filtered with a low-pass filter with cut-off frequencies f_c ranging from 0.05 to 1 Hz.

3. Results

3.1. Effect of additive Gaussian noise vs. mean stimulus level on signal transduction

Adding Gaussian noise (GN) to the subthreshold stimuli (Fig. 3a) leads to the generation of repetitive $[Ca^{2+}]_i$-spikes (Fig. 3b) at lower noise intensities and variances respectively than adding the mean level of the Gaussian noise ($\overline{GN}$) to the stimulus as a control (Fig. 3c,d). At higher noise variances, the behavior of transmembrane signal transduction from the extracellular stimulus to the $[Ca^{2+}]_i$-spikes were similar for additive GN and additive $\overline{GN}$ (Fig. 4). This phenomenon of enhanced transmembrane signal transduction by adding GN could be observed for all interpulse intervals used in the simulations (Fig. 5). The difference between adding GN and the respective $\overline{GN}$ with respect to the initiation of signal transduction declined with growing cut-off frequencies for the filtered GN. Higher cut-off frequencies led to GN with high-frequency oscillations around the $\overline{GN}$ which approximated $\overline{GN}$ more closely. We have proposed a mathematical model that allows for the on-line decoding of $[Ca^{2+}]_i$-spike trains into cellular responses represented by the

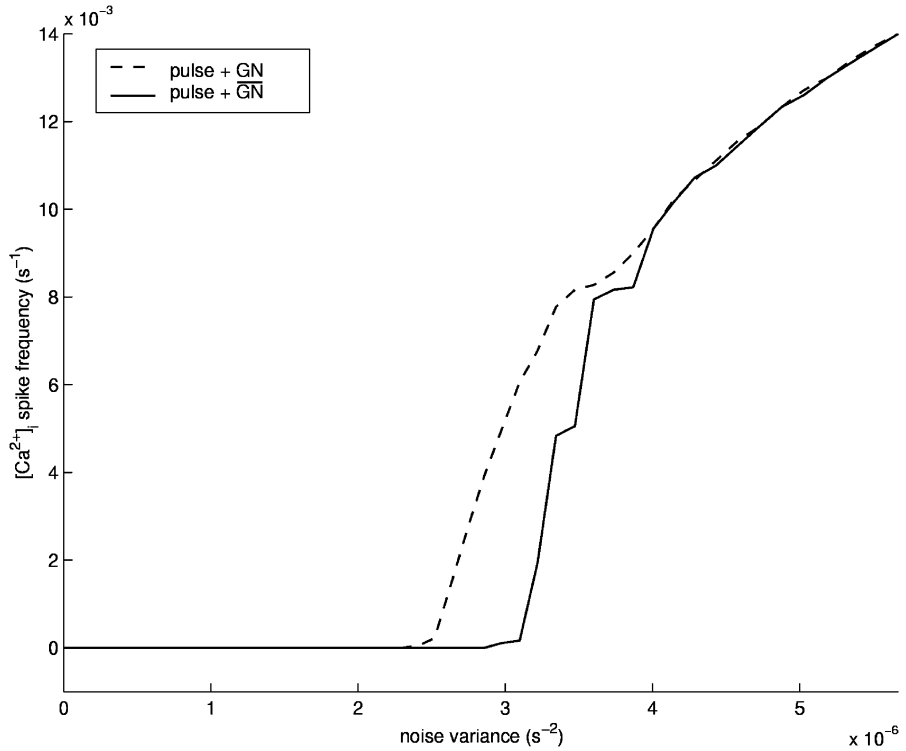

Fig. 4. Frequency of $[Ca^{2+}]_i$-spikes as a function of the noise variance. The stimuli were chosen as displayed in Fig. 3. Low levels of noise did not induce a transduction of the extracellular periodic stimulus into $[Ca^{2+}]_i$-oscillations. In all of the simulations the added GN led to earlier signal transduction than the corresponding $\overline{GN}$ (Fig. 5). The mean level of the additive noise is increasing with the variance.

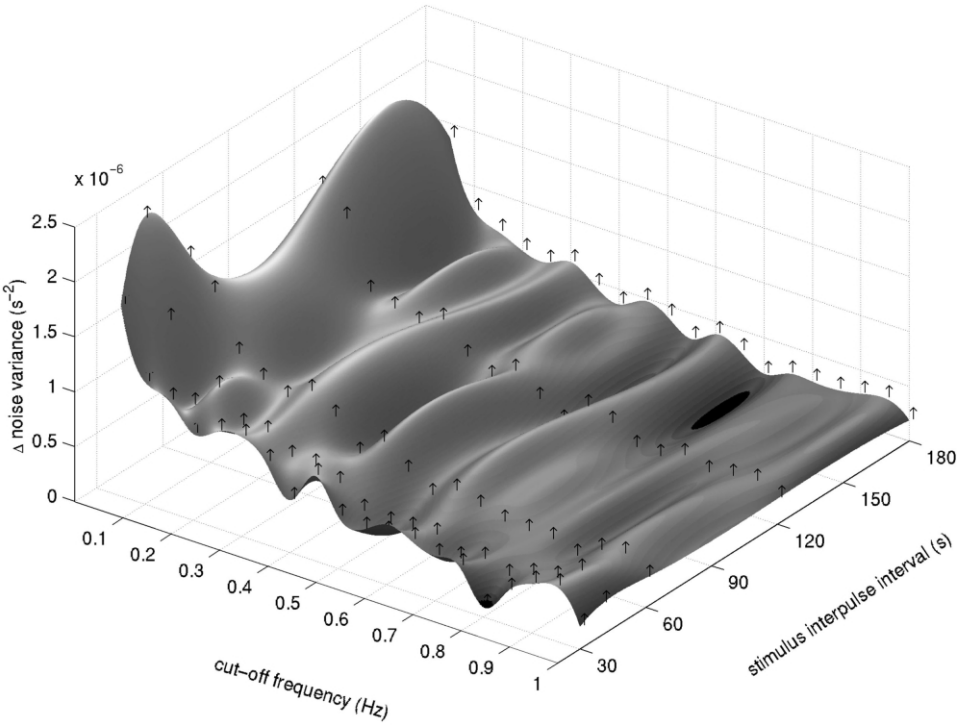

Fig. 5. Adding Gaussian noise (GN) to the subthreshold pulsatile stimulus leads to earlier signal transduction than adding a constant ($\overline{GN}$) with the same mean level as GN. This difference is expressed as the noise variance and is a function of the cut-off frequency of filtered GN and the interpulse interval of the periodic stimulus. This is a qualitative look on the systems behavior obtained by interpolation of the datapoints (origins of ↑).

activation of proteins [36]. Using this model to decode the simulated $[Ca^{2+}]_i$-spike trains into the phosphorylation of cellular target proteins we found an analogous behavior of enhanced signal transduction under additive GN compared to $\overline{GN}$ (data not shown).

3.2. Dynamical properties of the model for $[Ca^{2+}]_i$-oscillations

The dynamical structure of this model for $[Ca^{2+}]_i$-oscillations can be seen clearly in the bifurcation diagram which was produced as a function of k_g, the amplitude of the extracellular stimulus (Fig. 6). The AUTO program predicts two Hopf bifurcations, the left Hopf bifurcation (LHB) at $k_g = 0.008906$ and the right Hopf bifurcation (RHB) at $k_g = 0.044919$. Hopf bifurcations occur in two-dimensional systems when a stable fixed point becomes unstable to form a limit cycle, or a stable limit cycle becomes unstable to a fixed point as a control parameter is varied. Both LHB and RHB are subcritical. If the direction of the bifurcating branch is opposite to the direction at which stability of the main branch is lost, the branch is called subcritical and it is generally unstable.

In biological systems, subcritical Hopf bifurcations occur, e.g. in the dynamics of nerve cells [37]. The steady-state branch is shown by the dashed line and the oscillatory branch is shown by the solid line. In this study, it is of major interest to see what happens when GN is added in the area of LHB. Note that from LHB to the left periodic limit (LPL) $k_g = 0.008816$, there exists a bistable region. Also note that the periodic state rises sharply. These features make the system very sensitive to noise, i.e. when the stimulus

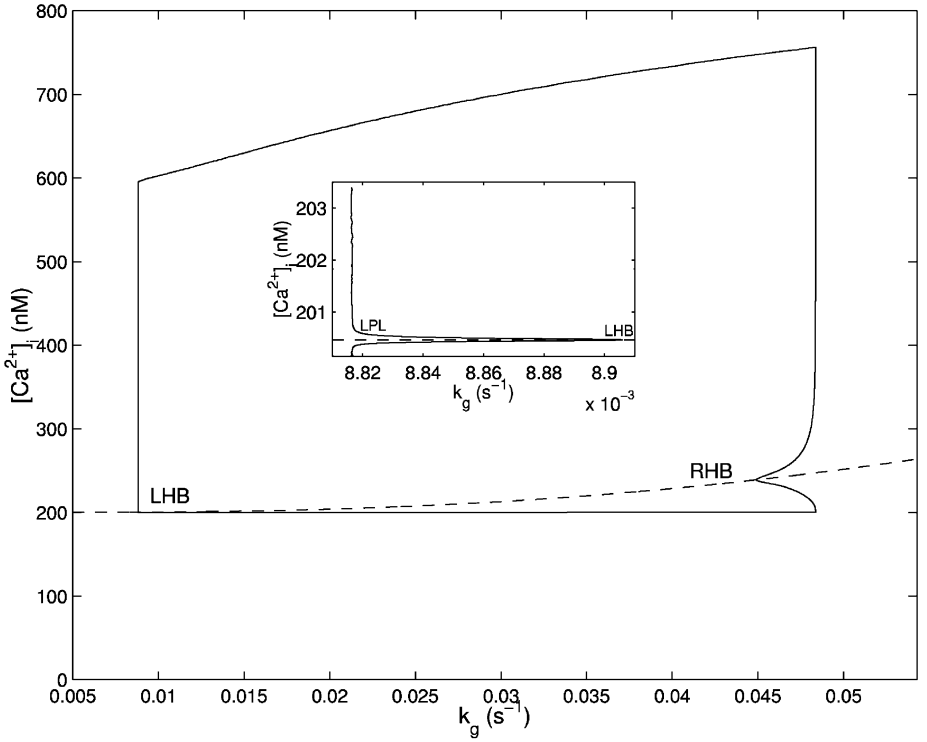

Fig. 6. Bifurcation analysis by the AUTO program showing the effect of the concentration of the agonist, k_g, on the generation of Ca^{2+}-spikes. The amplitude of $[Ca^{2+}]_i$ is plotted as a function of k_g. LHB and RHB are standing for left and right Hopf bifurcation. Inset shows lower left corner on an expanded scale.

strength plus noise passes slightly above the threshold stimulus (i.e. LPL), the model gives rise to a $[Ca^{2+}]_i$-spike in response to a hormone pulse.

4. Discussion

Besides its deterministic pulsatile structure, most temporal profiles of hormone concentrations and neurotransmitter levels exhibit endogenous noise caused by factors such as the secretory process itself or turbulence induced by the architecture of the blood vessel system. Traditionally, noise in biological information processing has been regarded as detrimental to information transfer.

In our numerical study of hormone induced $[Ca^{2+}]_i$-oscillations, we demonstrate that weak subthreshold stimuli only yield a cellular response by adding external GN, whereas adding the constant mean level ($\overline{GN}$) of noise does not exhibit this type of behavior. It has been shown experimentally that the frequencies of $[Ca^{2+}]_i$-transients occurring naturally optimally encode distinct aspects of neuronal differentiation and might implement an intrinsic developmental program [12,13]. The complex pattern of $[Ca^{2+}]_i$-transients found in our model situation fits to experimentally obtained data when applying weak external stimuli close to the threshold level [38]. Thus, the $[Ca^{2+}]_i$-patterns found in our simulations might mimic the physiologically occurring patterns of $[Ca^{2+}]_i$-transients.

Future experiments could investigate the effects of a varying signal amplitude on the GN amplitude required to effect signal transduction. In addition, future research on this topic might be based on a more elaborate model of the signal

transduction, e.g. by letting the receptor concentration dependence follow a saturation isotherm and not a linear function, as we used here, which holds only for ligand concentrations well below the dissociation constant for receptor–ligand binding.

Endogenous noise may not only improve the transduction of a single extracellular stimulus to the intracellular pathways by a cooperative effect between the deterministic and the stochastic signal; it may also function in the cooperative behavior of the 'cross talk' between apparently unrelated intracellular pathways and induce a cellular response to subthreshold stimuli. The understanding of malfunctioning in the interaction of these pathways leading to diseases such as diabetes and cancer is of major importance [39,40]. It will be necessary to test these predictions by investigating the impact of noise in hormonal systems on the cellular and subcellular level.

Acknowledgements

We thank the late Teresa Chay for help with the bifurcation analysis. Supported by Deutsche Forschungsgemeinschaft under grants Br 915/4-4 and Scho 466/1-3.

References

[1] E.D. Adrian, The Basis of Sensation, Norton, New York, 1928.
[2] S. Gammeltoff, C.R. Kahn, Hormone signaling via membrane receptors in: L.J. DeGroot (Ed.), Endocrinology, W.B. Saunders Company, Philadelphia, 1995, pp. 17–56.
[3] J. Levine, Pulsatility in neuroendocrine systems Acadamic Press, San Diego, Trends in Neurosciences, 20, 1994.
[4] G. Brabant, K. Prank, C. Schöfl, Pulsatile patterns in hormone secretion, Trends Endocrinol. Metab. 3 (1993) 183–190.
[5] E. Knobil, The neuroendocrine control of the menstrual cycle, Rec. Prog. Horm. Res. 36 (1981) 53–88.
[6] D.S. Weigle, C.J. Goodner, Evidence that the physiological pulse frequency of glucagon secretion optimizes glucose production by perifused rat hepatocytes, Endocrinology 118 (1986) 1606–1613.
[7] M.A. Shupnik, Effects of gonadotropin-releasing hormone on rat gonadotropin gene transcription in vitro: requirement for pulsatile administration for lutenizing hormone-beta gene stimulation, Mol. Endocrinol. 4 (1990) 1444–1450.
[8] M.J. Berridge, A. Galione, Cytosolic calcium oscillatos, FASEB J. 2 (1988) 3074–3082.
[9] M.D. Bootman, M.J. Berridge, The elemental principles of calcium signaling, Cell 83 (1995) 675–678.
[10] R.J. Colbran, T.R. Soderling, Calcium/calmodulin-dependent protein kinase II, Curr. Top. Cell. Regul. 31 (1990) 181–221.
[11] H. Bading, D.D. Ginty, M.E. Greenberg, Regulation of gene expression in hippocampal neurons by distinct calcium signaling pathways, Science 260 (1993) 181–186.
[12] X. Gu, E.C. Olson, N.C. Spitzer, Spontaneous neuronal calcium spikes and waves during early differentiation, J. Neurosci. 14 (1995) 6325–6335.
[13] X. Gu, N.C. Spitzer, Distinct aspects of neuronal differentiation encoded by frequency of spontaneous Ca^{2+} transients, Nature 375 (1995) 784–787.
[14] H.T. Cline, R.W. Tsien, Glutamate-induced increases in intracellular Ca^{2+} in cultured frog tectal cells mediated by direct activation of NMDA receptor channels, Neuron 6 (1991) 259–267.
[15] C. Schöfl, G. Brabant, R.D. Hesch, A. von zur Mühlen, P.H. Cobbold, K.S. Cuthbertson, Temporal patterns of alpha 1-receptor stimulation regulate amplitude and frequency of calcium transients, Am. J. Physiol. 265 (1993) C1030–C1036.
[16] T.R. Chay, Y.S. Lee, Y.S. Fan, Appearance of phase-locked Wenckebach-like rhythms, devil's staircase and universality in intracellular calcium spikes in non-excitable cell models, J. Theor. Biol. 174 (1995) 21–44.
[17] K.S.R. Cuthbertson, T.R. Chay, Modelling receptor-controlled intracellular calcium oscillators, Cell Calcium 12 (1991) 97–109.
[18] A. Longtin, A. Bulsara, F. Moss, Time-interval sequences in bistable systems and the noise-induced transmission of information by sensory neurons, Phys. Rev. Lett. 67 (1991) 656–659.
[19] A. Bulsara, E.W. Jacobs, T. Zhou, F. Moss, L. Kiss, Stochastic resonance in a single neuron model: theory and analog simulation, J. Theor. Biol. 152 (1991) 531–555.
[20] J.K. Douglass, L. Wilkens, E. Pantazelou, F. Moss, Noise enhancement of information transfer in crayfish mechanoreceptors by stochastic resonance, Nature 365 (1993) 337–340.
[21] F. Moss, A. Bulsara, M.F. Shlesinger, Proceedings of the NATO Advanced Research Workshop: Stochastic resonance in physics and biology, J. Statist. Phys. 70 (1993) 1–512.
[22] A.J. Longtin, Stochastic resonance in neuron models, J. Statist. Phys. 70 (1993) 309–327.
[23] K. Wiesenfeld, D. Pierson, E. Pantazelou, C. Dames, F. Moss, Stochastic resonance on a circle, Phys. Rev. Lett. 72 (1994) 2125–2129.
[24] J.J. Collins, C.C. Chow, T.T. Imhoff, Stochastic resonance without tuning, Nature 376 (1995) 236–238.

[25] B.J. Gluckman, T.I. Netoff, E.J. Neel, W.L. Ditto, M.L. Spano, S.J. Schiff, Stochastic resonance in a neuronal network from mammalian brain, Phys. Rev. Lett. 77 (1996) 4098–4101.
[26] S.M. Bezrukov, I. Vodyanoy, Noise-induced enhancement of signal transduction across voltage-dependent ion channels, Nature 378 (1995) 362–364.
[27] Y. Kashimori, H. Funakubo, T. Kambara, Effect of syncytium structure of receptor systems on stochastic resonance induced by chaotic potential fluctuation, Biophys. J. 75 (1998) 1700–1711.
[28] R. Benzi, A. Sutera, A. Vulpiani, The mechanism of stochastic resonance, J. Phys. A 14 (1981) L453–L457.
[29] J.P. Eckmann, L. Thomas, P. Wittwer, Intermittency in the presence of noise, J. Phys. A 14 (1981) 3153–3168.
[30] J.P. Eckmann, L. Thomas, Remarks on stochastic resonances, J. Phys. A 15 (1982) L261–L266.
[31] S. Fauve, F. Heslot, Stochastic resonance in a bistable system, Phys. Lett. A 97 (1983) 5–7.
[32] B. McNamara, K. Wiesenfeld, R. Roy, Observation of stochastic resonance in a ring laser, Phys. Rev. Lett. 60 (1988) 2626–2629.
[33] A. Simon, A. Libchaber, Escape and synchronization of a Brownian particle, Phys. Rev. Lett. 68 (1992) 3375–3378.
[34] K. Wiesenfeld, F. Moss, Stochastic resonance and the benefits of noise: from ice ages to crayfish and squids, Nature 373 (1995) 33–36.
[35] E.J. Doedel, AUTO: A program for the automatic bifurcation and analysis of autonomous systems, Cong. Num. 30 (1981) 265–284.
[36] K. Prank, L. Läer, A. von zur Mühlen, G. Brabant, C. Schöfl, Decoding of intracellular calcium spike trains, Europhys. Lett. 42 (1998) 143–147.
[37] J. Rinzel, G.B. Ermentrout, in: C. Koch, I. Segev (Eds.), Methods in Neuronal Modeling: From Synapses to Networks, MIT Press, Cambridge, MA, 1998, pp. 251–291.
[38] C. Schöfl, A. Sanchez-Bueno, G. Brabant, P.H. Cobbold, K.S. Cuthbertson, Frequency and amplitude enhancement of calcium transients by cyclic AMP in hepatocytes, Biochem. J. 273 (1991) 799–802.
[39] C. Schöfl, K. Prank, G. Brabant, Mechanisms of cellular information processing, Trends Endocrinol. Metab. 5 (1994) 53–59.
[40] G. Weng, U.S. Bhalla, R. Iyengar, Complexity in biological signaling systems, Science 284 (1999) 92–96.